# 17 The car axis problem

## 17.1 General information

The problem is a stiff DAE of index 3, consisting of 8 differential and 2 algebraic equations. It has been taken from [Sch94]. Since not all initial conditions were given, we have chosen a consistent set of initial conditions. The software part of the problem is in the file caraxis.f available at [MM08].

## 17.2 Mathematical description of the problem

The problem is of the form

$$p' = q, \tag{II.17.1}$$

$$Kq' = f(t,p,\lambda), \qquad p,q \in \mathbb{R}^4, \quad \lambda \in \mathbb{R}^2, \quad 0 \le t \le 3, \tag{II.17.2}$$

$$0 = \phi(t,p), \tag{II.17.3}$$

with initial conditions $p(0) = p_0$, $q(0) = q_0$, $p'(0) = q_0$, $q'(0) = q_0'$, $\lambda(0) = \lambda_0$ and $\lambda'(0) = \lambda_0'$.

The matrix $K$ reads $\varepsilon^2 \frac{M}{2} I_4$, where $I_4$ is the $4 \times 4$ identity matrix. The function $f : \mathbb{R}^7 \to \mathbb{R}^4$ is given by

$$f(t,p,\lambda) = \begin{pmatrix} (L_0 - L_l)\dfrac{x_l}{L_l} & +\lambda_1 x_b + 2\lambda_2 (x_l - x_r) \\ (L_0 - L_l)\dfrac{y_l}{L_l} & +\lambda_1 y_b + 2\lambda_2 (y_l - y_r) - \varepsilon^2 \dfrac{M}{2} \\ (L_0 - L_r)\dfrac{x_r - x_b}{L_r} & -2\lambda_2 (x_l - x_r) \\ (L_0 - L_r)\dfrac{y_r - y_b}{L_r} & -2\lambda_2 (y_l - y_r) - \varepsilon^2 \dfrac{M}{2} \end{pmatrix}.$$

Here, $(x_l, y_l, x_r, y_r)^{\mathrm{T}} := p$, and $L_l$ and $L_r$ are given by

$$\sqrt{x_l^2 + y_l^2} \quad \text{and} \quad \sqrt{(x_r - x_b)^2 + (y_r - y_b)^2}.$$

Furthermore, the functions $x_b(t)$ and $y_b(t)$ are defined by

$$x_b(t) = \sqrt{L^2 - y_b^2(t)}, \tag{II.17.4}$$

$$y_b(t) = h \sin(\omega t). \tag{II.17.5}$$

The function $\phi : \mathbb{R}^5 \to \mathbb{R}^2$ reads

$$\phi(t,p) = \begin{pmatrix} x_l x_b + y_l y_b \\ (x_l - x_r)^2 + (y_l - y_r)^2 - L^2 \end{pmatrix}.$$

The constants are listed below.

| | | | | | | | | | | | |
|---|---|---|---|---|---|---|---|---|---|---|---|
| $L$ | = | 1 | $\epsilon$ | = | $10^{-2}$ | $h$ | = | $10^{-1}$ | $\omega$ | = | 10 |
| $L_0$ | = | 1/2 | $M$ | = | 10 | $\tau$ | = | $\pi/5$ | | | |

Consistent initial values are

$$p_0 = \begin{pmatrix} 0 \\ 1/2 \\ 1 \\ 1/2 \end{pmatrix}, \quad q_0 = \begin{pmatrix} -1/2 \\ 0 \\ -1/2 \\ 0 \end{pmatrix}, \quad q_0' = \frac{2}{M\varepsilon^2} f(0, p_0, \lambda_0), \quad p_0' = q_0, \quad \lambda_0 = \lambda_0' = (0,0)^{\mathrm{T}}.$$

The index of the variables $p$, $q$ and $\lambda$ is 1, 2 and 3, respectively.

## 17.3 Origin of the problem

The car axis problem is an example of a rather simple multibody system, in which the behavior of a car axis on a bumpy road is modeled by a set of differential-algebraic equations.

A simplification of the car is depicted in Figure II.17.1. We model the situation that the left wheel

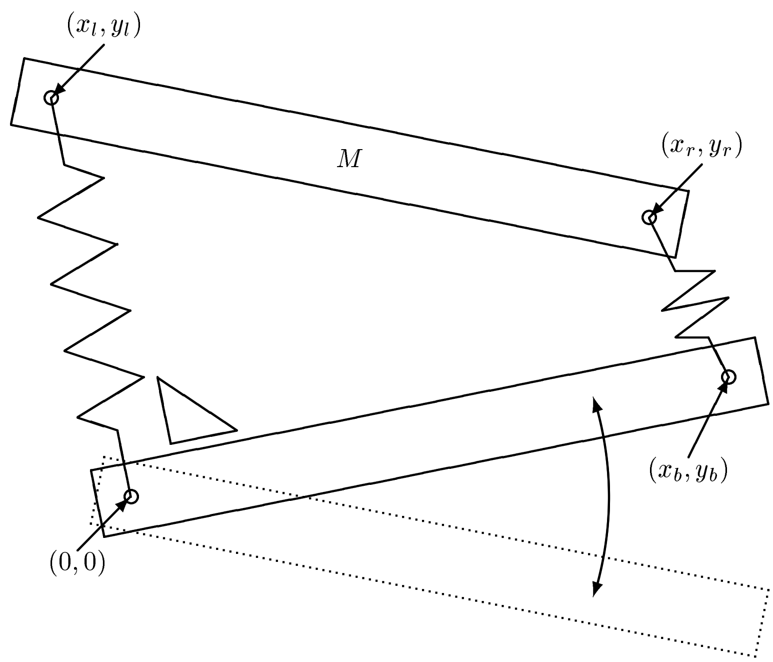


FIGURE II.17.1: *Modelnn of the car axis.*

at the origin $(0,0)$ rolls on a flat surface and the right wheel at coordinates $(x_b, y_b)$ rolls over a hill of height $h$ every $\tau$ seconds[2]. This means that $y_b$ varies over time according to (II.17.5). The length of the axis, denoted by $L$, remains constant over time, which means that $x_b$ has to fulfill (II.17.4). Two springs carry over the movement of the axis between the wheels to the chassis of the car, which is represented by the bar $(x_l, y_l)$–$(x_r, y_r)$ of mass $M$. The two springs are assumed to be massless and have Hooke's constant $1/\epsilon^2$ and length $L_0$ at rest.

There are two position constraints. Firstly, the distance between $(x_l, y_l)$ and $(x_r, y_r)$ must remain constantly $L$ and secondly, for simplicity of the model, we assume that the left spring remains orthogonal to the axis. If we identify $p$ with the vector $(x_l, y_l, x_r, y_r)^{\mathrm{T}}$, then we see that Equation (II.17.3) reflects these constraints.

Using Lagrangian mechanics, the equations of motions for the car axis are given by

$$\frac{M}{2}\frac{\mathrm{d}^2 p}{\mathrm{d}t^2} = F_{\mathrm{H}} + G^{\mathrm{T}}\lambda + F_{\mathrm{g}}. \tag{II.17.6}$$

Here, $G$ is the $2 \times 4$ Jacobian matrix of the function $\phi$ with respect to $p$ and $\lambda$ is the 2-dimensional vector containing the so-called Lagrange multipliers. The factor $M/2$ is explained by the fact that the mass $M$ is divided equally over $(x_l, y_l)$ and $(x_r, y_r)$. The force $F_{\mathrm{H}}$ represents the spring forces:

$$F_{\mathrm{H}} = -(\cos(\alpha_l)F_l, \sin(\alpha_l)F_l, \cos(\alpha_r)F_r, \sin(\alpha_r)F_r)^{\mathrm{T}},$$

[2] in the source fortran file the variable $r$ stands for $h$

where $F_l$ and $F_r$ are the forces induced by the left and right spring, respectively, according to Hooke's law:

$$F_l = (L_l - L_0)/\epsilon^2,$$
$$F_r = (L_r - L_0)/\epsilon^2.$$

Here, $L_l$ and $L_r$ are the actual lengths of the left and right spring, respectively:

$$L_l = \sqrt{x_l^2 + y_l^2},$$
$$L_r = \sqrt{(x_r - x_b)^2 + (y_r - y_b)^2}.$$

Furthermore, $\alpha_l$ and $\alpha_r$ are the angles of the left and right spring with respect to the horizontal axis of the coordinate system:

$$\alpha_l = \arctan(y_l/x_l),$$
$$\alpha_r = \arctan((y_r - y_b)/(x_r - x_b)).$$

Finally, $F_g$ represents the gravitational force

$$F_g = -(0,1,0,1)^{\mathrm{T}} \frac{M}{2} g.$$

The original formulation [Sch94] sets $g = 1$.

We rewrite (II.17.6) as a system of first order differential equations by introducing the velocity vector $q$, so that we obtain the first order differential equations (II.17.1) and

$$\frac{M}{2}\frac{\mathrm{d}q}{\mathrm{d}t} = F_{\mathrm{H}} + G^{\mathrm{T}}\lambda + F_{\mathrm{g}}. \tag{II.17.7}$$

Setting $f = F_{\mathrm{H}} + G^{\mathrm{T}}\lambda + F_g$, it is easily checked that multiplying (II.17.7) by $\varepsilon^2$ yields (II.17.2).

To arrive at a consistent set of initial values $p_0$, $q_0$ and $\lambda_0$, we have to solve the system of equations consisting of the constraint

$$\phi(t_0, p_0) = 0, \tag{II.17.8}$$

and the 1 up to $k-1$ times differentiated constraint (II.17.8), where $k$ is the highest variable index. To facilitate notation, we introduce $\tilde{p} := (t, p^{\mathrm{T}})^{\mathrm{T}}$ and its derivative $\tilde{q} := \frac{\mathrm{d}\tilde{p}}{\mathrm{d}t} = (1, q^{\mathrm{T}})^{\mathrm{T}}$. The Jacobian of $\phi$ with respect to $\tilde{p}$ will be denoted by $\tilde{G}$. Here, $k = 3$, yielding the additional conditions

$$\tilde{G}(\tilde{p}_0)\tilde{q}_0 = 0 \tag{II.17.9}$$

and

$$\phi_{\tilde{p}\tilde{p}}(\tilde{p}_0)(\tilde{q}_0, \tilde{q}_0) + \tilde{G}(\tilde{p}_0)\tilde{q}_0' = 0,$$

where $\phi_{\tilde{p}\tilde{p}}$ denotes the second derivative of $\phi$ with respect to $\tilde{p}$. Using (II.17.6) and the fact that the first component of $\tilde{q}_0'$ vanishes, the latter condition equals

$$\phi_{\tilde{p}\tilde{p}}(\tilde{p}_0)(\tilde{q}_0, \tilde{q}_0) + \frac{2}{M} G(p_0)\left(F_{\mathrm{H}}(p_0) + G^{\mathrm{T}}(p_0)\lambda_0 + F_{\mathrm{g}}(p_0)\right) = 0. \tag{II.17.10}$$

The equations (II.17.8)–(II.17.10) are solved for

$$
\begin{aligned}
x_r &= L,\\
x_l &= 0,\\
y_r &= y_l = L_0,\\
x'_r &= x'_l = -\frac{L_0}{L}\frac{2\pi}{\tau}h,\\
y'_r &= \frac{L^2\tau}{2\pi h\varepsilon^2 M}(2\lambda_1 - \lambda_2),\\
y'_l &= \frac{L^2\tau}{2\pi\varepsilon^2 hM}(2\lambda_2 - \lambda_1) \pm \frac{L}{\varepsilon}\sqrt{\frac{-8\lambda_2 + 2\lambda_1}{M}}.
\end{aligned}
$$

Choosing $\lambda_1 = \lambda_2 = 0$, we arrive at the initial conditions listed in §17.2,

TABLE II.17.1: *Reference solution at the end of the integration interval.*

| | | | |
|---|---|---|---|
| $y_1$ | $0.493455784275402809122 \cdot 10^{-1}$ | $y_6$ | $0.744686658723778553466 \cdot 10^{-2}$ |
| $y_2$ | $0.496989460230171153861$ | $y_7$ | $0.175568157537232222276 \cdot 10^{-1}$ |
| $y_3$ | $0.104174252488542151681 \cdot 10$ | $y_8$ | $0.770341043779251976443$ |
| $y_4$ | $0.373911027265361256927$ | $y_9$ | $-0.473688659084893324729 \cdot 10^{-2}$ |
| $y_5$ | $-0.770583684040972357970 \cdot 10^{-1}$ | $y_{10}$ | $-0.110468033125734368808 \cdot 10^{-2}$ |

## 17.4 Numerical solution of the problem

Tables II.17.1–II.17.2 and Figures II.17.2–II.17.3 present the reference solution at the end of the integration interval, the run characteristics, the behavior of some solution components over the integration interval and the work-precision diagrams, respectively. The reference solution was computed on using quadruple precision GAMD on an Alphaserver DS20E, with a 667 MHz EV67 processor. atol = rtol = $h_0 = 10^{-24}$. For the work-precision diagrams, we used: rtol = $10^{-(4+m/4)}$, $m = 0, 1, \ldots, 24$; atol = rtol; h0 = rtol for BIMD, GAMD, MEBDFDAE, MEBDFI, RADAU and RADAU5.

# References

[MM08] F. Mazzia and C. Magherini. *Test Set for Initial Value Problem Solvers, release 2.4.* Department of Mathematics, University of Bari and INdAM, Research Unit of Bari, February 2008. Available at http://www.dm.uniba.it/~testset.

[Sch94] S. Schneider. *Intégration de systèmes d'équations différentielles raides et différentielles-algébriques par des méthodes de collocations et méthodes générales linéaires.* PhD thesis, Université de Genève, 1994.

TABLE II.17.2: *Run characteristics.*

| solver | rtol | atol | h0 | mescd | scd | steps | accept | #f | #Jac | #LU | CPU |
|---|---|---|---|---|---|---|---|---|---|---|---|
| BIMD | $10^{-4}$ | $10^{-4}$ | $10^{-4}$ | 2.19 | 0.34 | 71 | 71 | 1693 | 71 | 71 | 0.0088 |
| | $10^{-7}$ | $10^{-7}$ | $10^{-7}$ | 5.47 | 3.34 | 138 | 138 | 4511 | 138 | 138 | 0.0224 |
| | $10^{-10}$ | $10^{-10}$ | $10^{-10}$ | 8.01 | 5.35 | 235 | 235 | 9669 | 235 | 235 | 0.0488 |
| GAMD | $10^{-4}$ | $10^{-4}$ | $10^{-4}$ | 1.98 | 0.39 | 39 | 39 | 2169 | 39 | 39 | 0.0088 |
| | $10^{-7}$ | $10^{-7}$ | $10^{-7}$ | 4.82 | 2.64 | 98 | 98 | 7167 | 98 | 98 | 0.0293 |
| | $10^{-10}$ | $10^{-10}$ | $10^{-10}$ | 6.50 | 3.84 | 179 | 179 | 18771 | 179 | 179 | 0.0742 |
| MEBDFI | $10^{-4}$ | $10^{-4}$ | $10^{-4}$ | 0.88 | $-0.23$ | 280 | 278 | 1246 | 27 | 27 | 0.0059 |
| | $10^{-7}$ | $10^{-7}$ | $10^{-7}$ | 4.65 | 3.34 | 650 | 648 | 2797 | 47 | 47 | 0.0137 |
| | $10^{-10}$ | $10^{-10}$ | $10^{-10}$ | 4.21 | 2.08 | 1393 | 1391 | 5624 | 85 | 85 | 0.0264 |
| PSIDE-1 | $10^{-4}$ | $10^{-4}$ | | 0.83 | $-0.28$ | 55 | 54 | 1403 | 42 | 220 | 0.0098 |
| | $10^{-7}$ | $10^{-7}$ | | 4.41 | 2.27 | 179 | 172 | 4103 | 83 | 464 | 0.0273 |
| | $10^{-10}$ | $10^{-10}$ | | 7.25 | 4.86 | 625 | 612 | 13751 | 115 | 964 | 0.0869 |
| RADAU | $10^{-4}$ | $10^{-4}$ | $10^{-4}$ | 1.34 | 0.19 | 98 | 97 | 850 | 95 | 98 | 0.0039 |
| | $10^{-7}$ | $10^{-7}$ | $10^{-7}$ | 3.73 | 2.51 | 289 | 288 | 2559 | 282 | 288 | 0.0127 |
| | $10^{-10}$ | $10^{-10}$ | $10^{-10}$ | 5.99 | 4.22 | 179 | 178 | 4281 | 169 | 179 | 0.0166 |

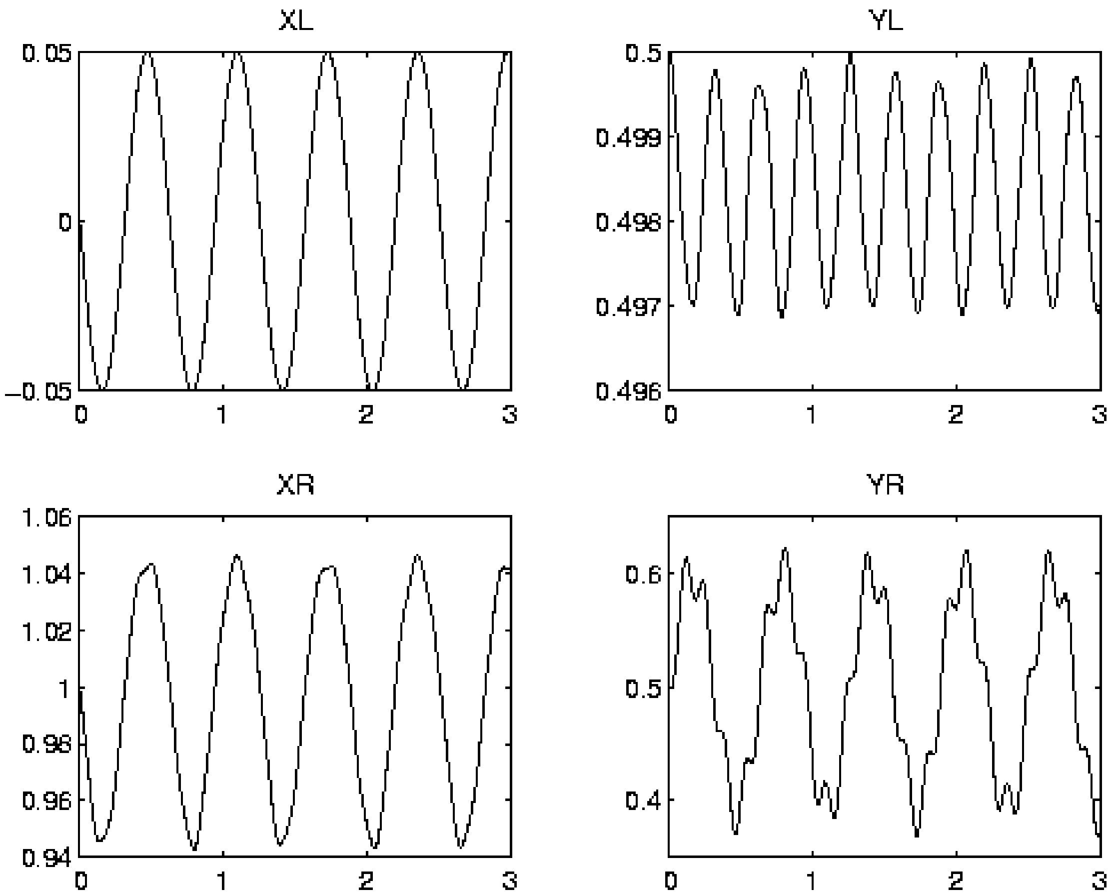


FIGURE II.17.2: *Behavior of* $(x_l, y_l)$ *and* $(x_r, y_r)$ *over the integration interval.*

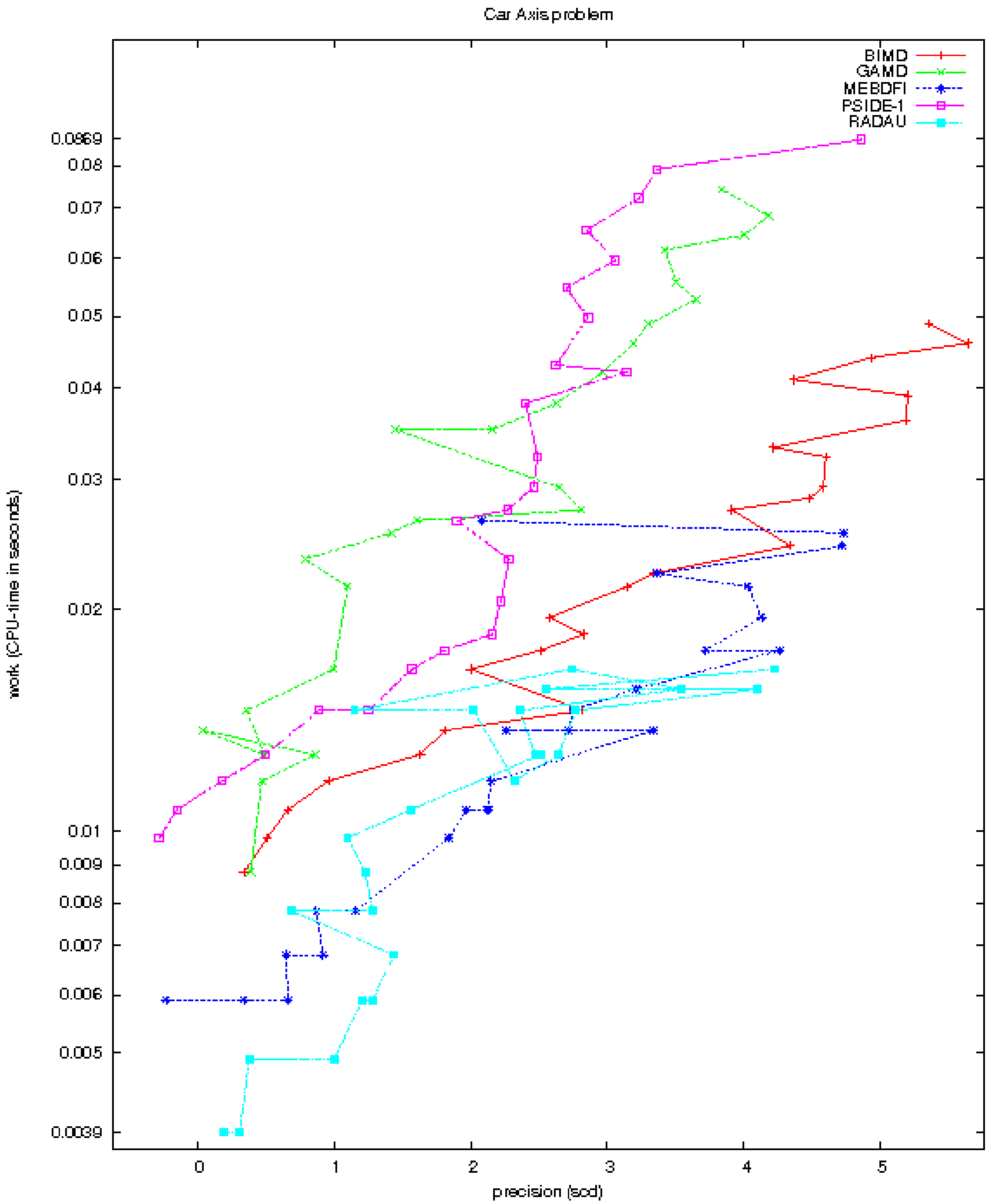


FIGURE II.17.3: *Work-precision diagram (scd versus CPU-time).*

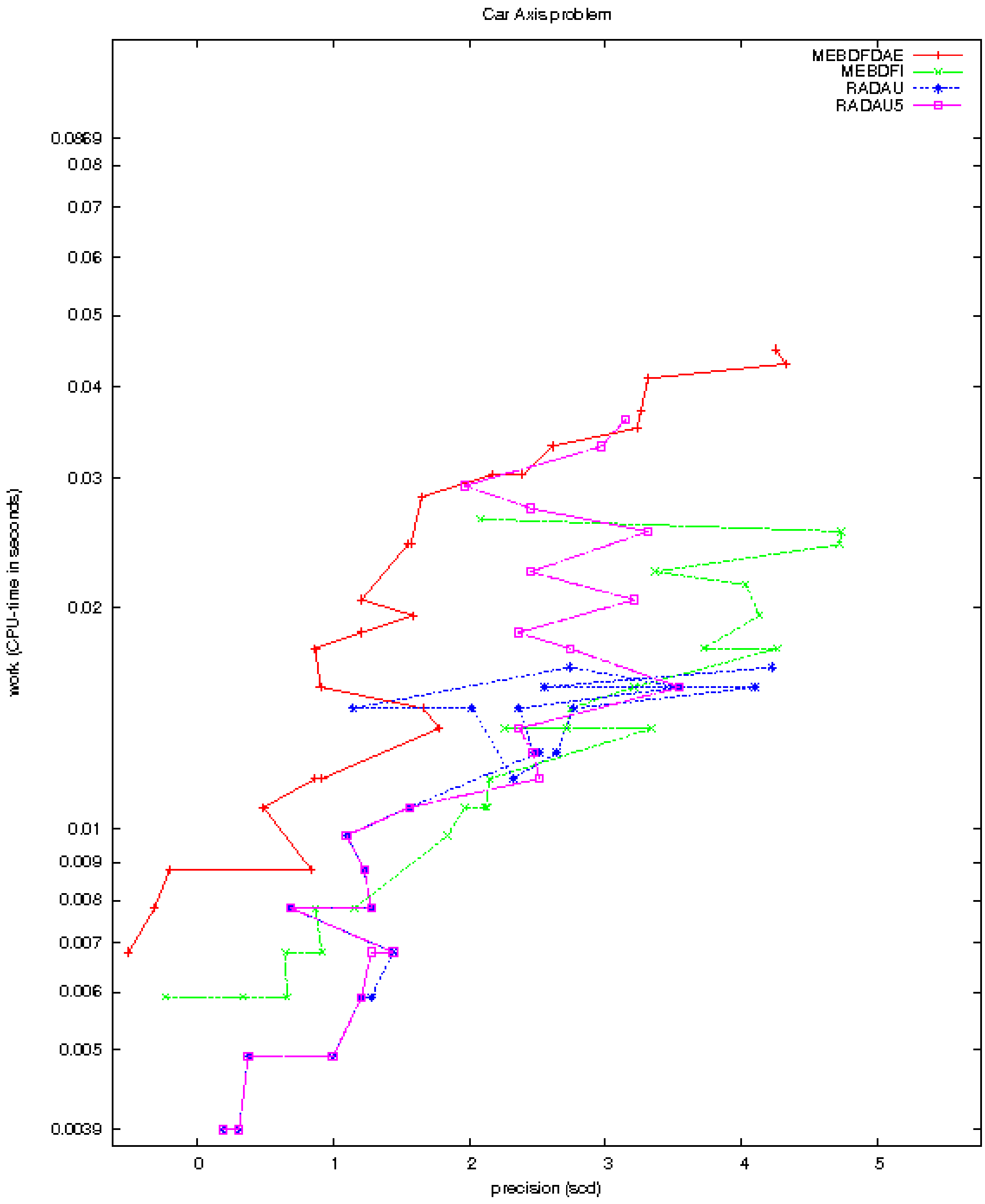


FIGURE II.17.4: *Work-precision diagram (scd versus CPU-time).*

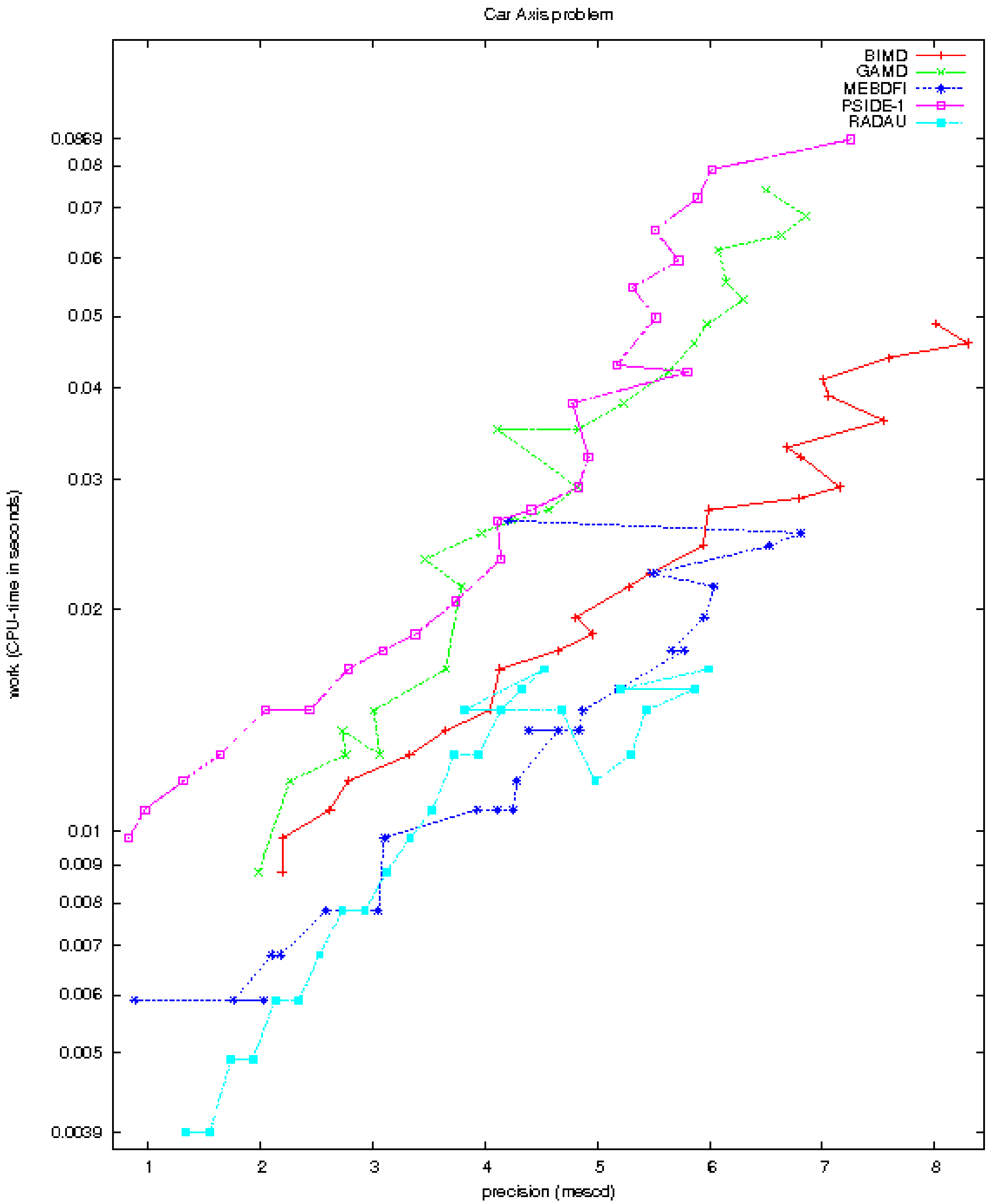


FIGURE II.17.5: *Work-precision diagram (mescd versus CPU-time).*

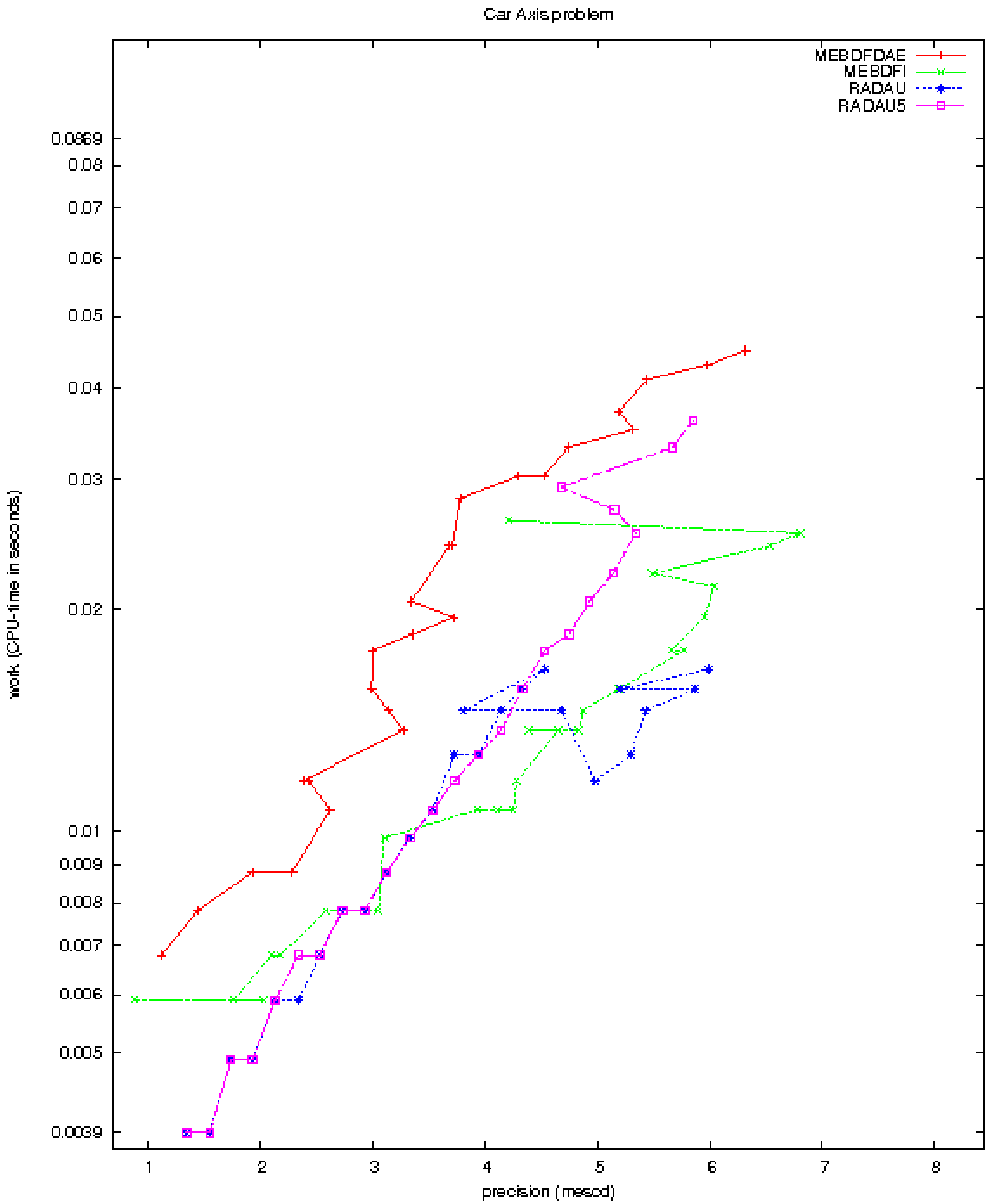


FIGURE II.17.6: *Work-precision diagram (mescd versus CPU-time).*